creative commons
COMMONS DEED

저작자표시-비영리-변경금지 2.0 대한민국

이용자는 아래의 조건을 따르는 경우에 한하여 자유롭게

- 이 저작물을 복제, 배포, 전송, 전시, 공연 및 방송할 수 있습니다.

다음과 같은 조건을 따라야 합니다:

저작자표시. 귀하는 원저작자를 표시하여야 합니다.

비영리. 귀하는 이 저작물을 영리 목적으로 이용할 수 없습니다.

변경금지. 귀하는 이 저작물을 개작, 변형 또는 가공할 수 없습니다.

- 귀하는, 이 저작물의 재이용이나 배포의 경우, 이 저작물에 적용된 이용허락조건을 명확하게 나타내어야 합니다.
- 저작권자로부터 별도의 허가를 받으면 이러한 조건들은 적용되지 않습니다.

저작권법에 따른 이용자의 권리는 위의 내용에 의하여 영향을 받지 않습니다.

이것은 이용허락규약(Legal Code)을 이해하기 쉽게 요약한 것입니다.

Disclaimer

dCollection

농학석사학위논문

Rice stripe virus 단백질 NS3 의 자가상호작용과 유전자 침묵 억제 기능에 중요한 아미노산 및 도메인의 동정

Identification of crucial residues or domain(s) of rice stripe virus NS3 protein required for self-interaction and for silencing suppressor activity

2016 년 2 월

서울대학교 대학원

농생명공학부 식물미생물학 전공

김한길

A THESIS FOR DEGREE OF MASTER SCIENCE

Identification of crucial residues or domain(s) of rice stripe virus NS3 protein required for self-interaction and for silencing suppressor activity

BY

Hangil Kim

Department of Agricultural Biotechnology

The Graduate School of Seoul National University

February 2016

ABSTRACT

Identification of crucial residues or domain(s) of rice stripe virus NS3 protein required for self-interaction and for silencing suppressor activity

Hangil Kim

Major in Plant Microbiology

Department of Agricultural Biotechnology

The Graduate Scholl of Seoul National University

Rice stripe virus (RSV), a member of the genus *Tenuivirus*, is one of the most harmful virus in rice cultivation. The genome of RSV consists of four single-stranded RNAs and encodes seven viral proteins. NS3, which is encoded from the RNA segment 3, was previously reported as a gene silencing suppressor for RNA silencing and self-interaction of NS3 is necessary for maintaining suppressor activity. To identify the crucial amino acid residues or domains(s) required for self-interaction of NS3, I used protein structure prediction program

and constructed eleven NS3 mutant clones including four alpha-helix deletion and substitution mutants. With these mutated clones, yeast-two hybrid (Y2H) and bimolecular fluorescence complementation (BiFC) assays were conducted for interaction study. Y2H and BiFC results showed that the N-terminal region of NS3 is essential for self-interaction. All of alpha-helix deletion mutants and substitution mutants lost its self-interaction ability in Y2H and BiFC assays. To identify the relationship between NS3 self-interaction and silencing suppressor activity, we used GFP silencing system in *Nicotiana benthamiana* with *Agrobacterium*-mediated transient overexpression of each mutated NS3 protein. All the deletion and four alpha-helix substitution mutations resulted in the loss of the silencing suppressor ability except lysine77 substitution mutation which maintained self-interaction capacity. Altogether, these results suggest that the NS3-NS3 self-interaction might be necessary for maintaining suppressor activity as a counter defense to RNA silencing system of the host plant.

Keywords: Rice stripe virus, Protein 3D structure prediction, RNA silencing, Viral Suppressor of RNA silencing (VSR), Protein-protein interaction (PPI), GFP silencing

Student number: 2014-21906

CONTENTS

Page

LIST OF TABLES

Page

LIST OF FIGURES

Page

INTRODUCTION

Plant viruses infect various important crops and cause severe economic losses. Rice stripe disease (RSD) caused by the rice stripe virus (RSV), a genus *Tenuivirus* (Pringle, 1998) is one of the most lethal diseases in rice cultivation. RSD caused 30~40% yield losses in the middle and lower regions of Yangtze River in China (Wu et al., 2009), and even caused more than 80% of loss in rice yield (Qu et al., 1997). RSD is dispersed in East Asian countries such as China, Japan, and Korea (Wu et al., 2014). The genome of RSV consists of four RNA segments encoding seven viral proteins. RNA1, which is the largest RNA, encodes RNA dependent RNA polymerase (RdRp) in viral-complementary sense RNA1 (vcRNA1) and the other three RNA segments encode six viral proteins using ambisense strategy (Lian et al., 2011). RNA2 encodes NS2 and NSvc2 protein which are reported as gene silencing suppressor and membrane associated protein, respectively (Du et al., 2011, Zhao et al., 2015). NS3 protein, which is encoded in viral sense RNA3 (vRNA3), is known as gene silencing suppressor (Xiong et al., 2009) and nucleocapsid protein (NP) is also encoded in vcRNA3 (Hayano et al., 1990). RNA4 encodes a disease specific protein (NCP) and movement protein (MP) in vRNA4 and vcRNA4, respectively (Wu et al., 2013).

Plants have been developed RNA silencing mechanisms against viral infection. Through the RNA silencing, plants prevent virus infection in transcriptional or post-transcriptional manner (Zhang et al., 2015). Small interfering RNAs (siRNAs) generated by viral infection induce the composition of RNA induced silencing complex (RISC) with Argonaute proteins (Guo et al., 2014). This RISC complex digests viral double-stranded RNAs (dsRNAs) or contributes to viral DNA methylation to repress virus replication (Wang et al., 2012).

As a counter defense to RNA silencing, viruses encodes viral suppressors of RNA silencing (VSRs) to attenuate or overcome the defense system of the plant hosts (Pumplin & Voinnet, 2013). Up to these days, numerous VSRs have been reported and their functions also have been identified. For example, tomato bushy stunt virus (TBSV) protein P19, mostly well-known silencing suppressor against to RNA silencing in plants, affects post transcriptional gene silencing mechanism. It is reported that P19 dimer prevent the composition of RISC by binding to siRNA. It also promotes the expression of miR168, which represses the translation of AGO1 protein (Danielson & Pezacki, 2013).

Some siRNA-binding VSRs, such as tobacco etch virus (TEV) HC-Pro, beet yellow virus (BYV) P21, tobamovirus P130, inhibit the 2'-O methylation on 3'-end of small RNAs, thereby RISC formation is inhibited (Guo et al., 2014). Furthermore, the functional analysis of the rice hoja blanca virus (RHBV) NS3 showed that the NS3 protein of RHBV represses RNA silencing mechanism of its host plant by directly binding to small RNAs (Hemmes et al., 2009).

The protein-protein interaction contributes to all of biological processes including translation process, transcription, enzymatic activity, signal transduction, protein synthesis and so on (Edwards & Wilson, 2011). Especially, the interactions among the viral proteins and between viral proteins and host-factors are most significant factor regulating and/or affecting virus infection cycle in infected host (Guo et al., 2001).

In previous studies, the interactions of several VSRs identified. For example, TBSV P19 protein composes a homodimer to bind to siRNA (Park et al., 2004). In addition, tomato aspermy virus (TAV) 2b protein also reported for its self-interaction and formation of homodimer. RHBV NS3 also forms homodimer and binds to siRNA duplex to repress PTGS induced by siRNA (Guo et al., 2014).

For RSV proteins, the interaction between RdRp and NP was reported (Zhao et al., 2015). Furthermore, self-interaction of NP and its crucial amino acids were also identified (Lian et al., 2014). Likewise, the self-interaction of RSV NS3 was reported and functional study of this protein as a RNA silencing suppressor was also conducted (Xiong et al., 2009). However, the crucial amino acids or motif(s) required for the NS3 self-interaction was not identified and the relationship between NS3 self-interaction and silencing suppressor activity is still unidentified.

In this study, interaction study of RSV NS3 was conducted by introducing mutations on to NS3 to identify the crucial amino acid or motif for self-interaction of NS3. Furthermore, with these mutated NS3s, silencing suppressor activity was investigated by using GFP silencing system in *Nicotiana benthamiana*. This study showed the crucial motifs required for the self-interaction of RSV NS3. I also identified the relationship between self-interaction of RSV NS3 and its function as a VSR.

MATERIAL AND METHODS

1. NS3 three-dimensional (3D) structure prediction

To identify NS3 self-interaction motifs, protein structure prediction program was used. For predition of NS3 full-length, N-terminal region of NS3 (aa 1–108), four alpha helix deletion mutants (NS3-ΔH1–4), four alpha helix substitution mutants (NS3-SUB1–4) and NS3-SUBK77A, I used I-TASSER server from Zhang Lab (http://zhanglab.ccmb.med.umich.edu/I-TASSER/). After that, PDB files provided by this program were downloaded and visualized by using UCSF Chimera program.

2. Construction of RSV NS3 mutants

RSV NS3 coding sequence was amplified from previously constructed plasmid which contains RSV-RNA3 (GenBank: FJ602681). Polymerase chain reaction (PCR) was conducted with PfuUltra II Fusion HS DNA Polymerase (Agilent Technologies, USA) and NS3 specific primer-pair (NS3-F/R). Forward primer contains CACC on 5' end for directional cloning to pENTR/D-TOPO vector. The PCR product was purified with NucleoSpin Gel and PCR Clean-up (Macherey-Nagel, Germany) and then directly cloned into pENTR/D-TOPO vector (Invitrogen, USA) following manufacturer's instruction.

To generate N-terminal region and C-terminal region of NS3, PCR was conducted with pENTR-NS3 as a template, and also NS3-F/NS3(108)-R or NS3(109)-F/NS3-R primer pairs were used for amplification of N-terminal or C-terminal region, respectively (Table 1). For

construction of alpha-helix deletion mutants, single-joint PCR (SJ-PCR) was conducted with six primers (Table 2). Likewise, alanine-substitution mutants were also generated with six primers for each mutant (Table 2 and 3). For construction of alpha-helix deletion mutants, RSV NS3 containing pENTR/D-TOPO plasmid was used as a template and PCR was conducted with Ex-Taq DNA polymerase (Takara, Japan) and primer-pairs (M13-forward/NS3-DEL-R and M13-reverse/NS3-DEL-F primer-pairs) were used for amplification of 5′ fragment and 3′ fragment, respectively. For substitution mutants, M13-forward/NS3-SUB-R and M13-reverse/NS3-SUB-F primer-pairs were used. Each amplified PCR products of partial NS3 fragments were purified by gel-extraction with NucleoSpin Gel and PCR Clean-up kit. PCR products covering the regions from M13-forward primer binding site to NS3 alpha-helix deletion/substitution site and from NS3 alpha-helix deletion/substitution site to M13-reverse primer binding site were used for second round PCR. The second round PCR products were directly used as templates for the final round PCR using NS3-F primer containing CACC on 5′ end and NS3-R primer. To amplify final PCR product with blunt end, PfuUltra II Fusion HS DNA Polymerase was used.

Table 1. List of primers for amplification of NS3-ΔC and NS3-ΔN mutants.

Mutant	Primers	Sequences	Region
NS3-△C	NS3-F	CACCATGAACGTGTTCACATCGTCTG	aa 1-108
	NS3-108-R	CTAGAAGAACTTCACATATGAGGATGAC	
NS3-△N	NS3-109-F	CACCATGACTGAAGTGAAGCCAAGACC	aa 109-212
	NS3-R	CTACAGCACAGCTGGAGAGATG	

Table 2. List of primers for construction of alpha-helix deletion mutants. Each primers for deletion mutant contains flanking region for single joint PCR.

Mutant	Primer	Sequence
NS3-△H1	NS3-DEL1-F	TAAACTGTGATGATGTCCATTGTTCTAGGCACCCTTCCATTG
	NS3-DEL1-R	CAATGGAAGGGTGCCTAGAACAATGGACATCATCACAGTTTA
NS3-△H2	NS3-DEL2-F	CTAGGCACCCTTCCATTGATCATGGCCCTGATGATGCTG
	NS3-DEL2-R	CAGCATCATCAGGGCCATGATCAATGGAAGGGTGCCTAG
NS3-△H3	NS3-DEL3-F	CTTCTTCATGGCCCTGATGATTCCCATGATAAGAATCTCCCA
	NS3-DEL3-R	TGGGAGATTCTTATCATGGGAATCATCAGGGCCATGAAGAAG
NS3-△H4	NS3-DEL4-F	GATAAGAATCTCCCAGAAGAGTACTTCTTCACTGAAGTGAAGCCAA
	NS3-DEL4-R	TTGGCTTCACTTCAGTGAAGAAGTACTCTTCTGGGAGATTCTTATC
	M13-F(-20)	GTAAAACGACGGCCAG
	M13-R	CAGGAAACAGCTATGAC

Table 3. List of primers for construction of alanine-substitution mutants. Each primer contains flanking region for single joint PCR and alanine codon sequences.

Mutant	Primer	Sequence
NS3-SUB1	NS3-SUB1-F	CTGTGATGATGTCCATTGTGCAGCAGCAGCAGCAGCAGCAGCAGCA
		GCAGCAGCAGCATCTAGGCACCCTTCCAT
	NS3-SUB1-R	ATGGAAGGGTGCCTAGATGCTGCTGCTGCTGCTGCTGCTGCTGC
		TGCTGCTGCACAATGGACATCATCACAG
NS3-SUB2	NS3-SUB2-F	GGCACCCTTCCATTGATGCAGCAGCAGCAGCAGCAGCAGCACATGG
		CCCTGATGATG
	NS3-SUB2-R	CATCATCAGGGCCATGTGCTGCTGCTGCTGCTGCTGCATCAATG
		GAAGGGTGCC
NS3-SUB3	NS3-SUB3-F	CTTCATGGCCCTGATGATGCAGCAGCAGCAGCAGCAGCAGCAGCAG
		CAGCAGCAGCAGCAGCATCCCATGATAAGAATCTCC
	NS3-SUB3-R	GGAGATTCTTATCATGGGATGCTGCTGCTGCTGCTGCTGCTGCT
		GCTGCTGCTGCTGCTGCATCATCAGGGCCATGAAG
NS3-SUB4	NS3-SUB4-F	ATAAGAATCTCCCAGAAGAGTACGCAGCAGCAGCAGCAGCAGCAG
		CAGCAGCAGCAGCAGCATTCTTCACTGAAGTGAAGCC
	NS3-SUB4-R	GGCTTCACTTCAGTGAAGAATGCTGCTGCTGCTGCTGCTGCTGC
		TGCTGCTGCTGCGTACTCTTCTGGGAGATTCTTAT
NS3-SUB77	NS3-SUB77-F	GGCTCCTTCTTGGCAACTCTGATCTG
	NS3-SUB77-R	CAGATCAGAGTTGCCAAGAAGGAGCC

3. Vector construction and cloning

Each mutated NS3 amplicons were purified by gel extraction and directly cloned into the pENTR/D-TOPO vector following the manufacturer's instructions. To construct expression clones for Y2H, each mutated NS3s were inserted in pDEST32 (bait) and pDEST22 (prey) by *in vitro* recombination using Gateway LR Clonase II (Invitrogen, USA).

To generate BiFC clones, pSAT4-DEST-nEYFP-C1 and pSAT5-DEST-cEYFP-C1, which are containing N-terminal region or C-terminal region of yellow fluorescence protein (nYFP or cYFP), were modified. pSAT4-DEST-nEYFP-C1 and pSAT5-DEST-cEYFP-C1 vectors were digested with *Sce*I and *Ceu*I, respectively, and two constructs were ligated into pPZP vector after digestion with *Sce*I or *Ceu*I. By these steps, pPZP-DEST-nEYFP-C1 and pPZP-DEST-cEYFP-C1 vectors were generated and each mutated NS3 amplicons were inserted into these vectors by *in vitro* recombination using Gateway LR Clonase II.

4. Yeast two hybrid (Y2H) analysis

The pDEST32 and pDEST22 containing mutated NS3s were co-transformed into yeast strain MaV203 and then spreaded on SC-Leu-Trp (SC-LT) plates according to manufacturer's instruction. Each mutated NS3 transformants were selected by dropping diluted colonies on SC plates lacking Leu, Trp and His with 20mM 3AT (SC-LTH+3AT) and SC plates lacking Leu, Trp and Uracil (SC-LTU). As a control, pEXP32/Krev1 (bait), pEXP22/RalGDS-wt (prey), pEXP22/RalGDS-m1 (prey) and pEXP22/RalGDS-m2 (prey) plasmids which were provided by the ProQuest Two-hybrid System (Invitrogen) were used. RalGDS-wt strongly interacts with Krev1, but the interaction between Krev1 and RalGDS-m1 or RalGDS-m2 are weak or

not detectable, respectively. X-gal assay was conducted based on guideline of ProQuest Two-hybrid System (Invitrogen).

5. Bimolecular fluorescence complementation (BiFC) assay

For BiFC assay, pPZP-DEST-nEYFP-C1 and pPZP-DEST-cEYFP-C1 vectors containing mutated NS3s were transformed to *Agrobacterium tumefaciens* strain GV2260 by heat-shock method. Each expression clones were cultured in YEP medium containing rifampicin and spectinomycin antibiotics for 1 day and harvested by centrifugation. Harvested cells were resuspended on MMA medium (10mM $MgCl_2$, 10mM MES salt and 0.2mM acetosyringone) to an optical density (O.D) at 600 nm of 0.5. Resuspended cells were incubated at 28℃ for 2 hours with shaking and agroinfiltration was conducted with nYFP expression clone, cYFP expression clone and pTBSV-p19 into *N. benthamiana* leaves using 1 ml syringe without a needle. *N. benthamiana* plants were grown in a growth chamber in a condition of a 16/8 light/night period. Three days after agroinfiltration, YFP signal was observed by fluoresent microscopy (Carl Zeiss, Germany).

6. RNA silencing suppression analysis

To identify RNA silencing suppressor activity of NS3 mutants, mutated NS3s were cloned into pMDC32 vector. *in vitro* recombination using Gateway LR Clonase II was conducted for construction of mutated NS3 over-expression clones. In addition, for construction of GFP silencing clone, hairpin RNA construct of GFP, which contains two complementary GFP

partial sequences and intron of N gene from *Nicotiana glutinosa*, was generated. This hairpin GFP construct was ligated into pCAMBIA-0380 with T4 DNA ligase (Promega, USA) after digestion with *Sma*I. For *Agrobacterium*-mediated over-expression, each vectors were transformed into *A. tumefaciens* strain GV2260. For GFP over-expression, pPZP-SGFP clone, which is pPZP212 vector including GFP sequence, was used.

RESULTS

1. 3D structure prediction of RSV NS3 protein

The 3D structure of RSV NS3 protein was predicted with I-TASSER program and PDB files, which was provided by I-TASSER server, were visualized with UCSF Chimera program. RSV NS3 protein contains four alpha-helices, and these were located at the N-terminal region of NS3 peptides (aa 1–110) (Fig. 1, left). Furthermore, The 3D structure of NS3 N-terminal region (C-terminal deletion mutant) was also predicted with I-TASSER program and four alpha-helices were conserved at this peptide sequence (Fig. 1, right). Based on NS3 3D structure prediction model, NS3 C-terminal deletion mutant (aa 1–108) and N-terminal deletion mutant (aa 109–212) was constructed by PCR (Fig. 3). Four alpha-helices consist of amino acid 37–50, 56–63, 69–83 and 91–110.

2. Generation of NS3-mutants

Based on 3D structure of RSV NS3 peptide, four alpha-helix deletion mutants including NS3-ΔH1 (Δaa 37–50), NS3-ΔH2 (Δaa 56–63), NS3-ΔH3 (Δaa 69–83) and NS3-ΔH4 (Δaa 91–110) were designed and generated by single joint PCR (Fig. 3). Furthermore, to minimize configurational changes by deletion of alpha-helices, four alpha-helix substitution mutants were also generated by replacing amino acids, which consist of each alpha-helix, to alanines. Alanine is non-bulky, and substitution with alanine removes the specificity of each residues (Morrison & Weiss, 2001). In addition, the substitution with alanine minimizes the

configurational changes of peptides. The 3D structure predictions showed that four alpha-helices were conserved in each alpha-helix substitution mutants (Fig. 2). Additionally, single point mutation on K77, which is an unique charged amino acid in alpha-helix 3, was conducted by alanine substitution (NS3-K77A) (Fig. 3).

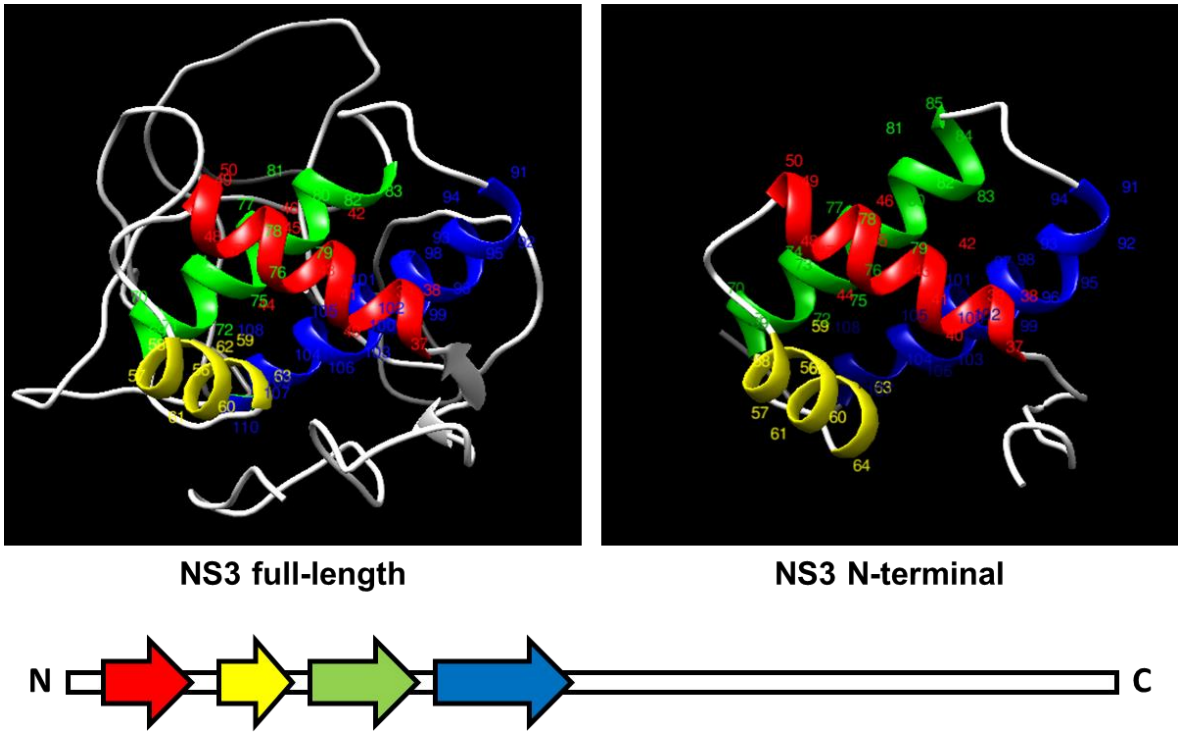

Fig. 1. Predicted 3D structure of NS3 and N-terminal portion of NS3. Four alpha-helices according to aa 37−50, aa 56−63, aa 69−83 and aa 91−110 were identified and these were still remained with out C-terminal region.

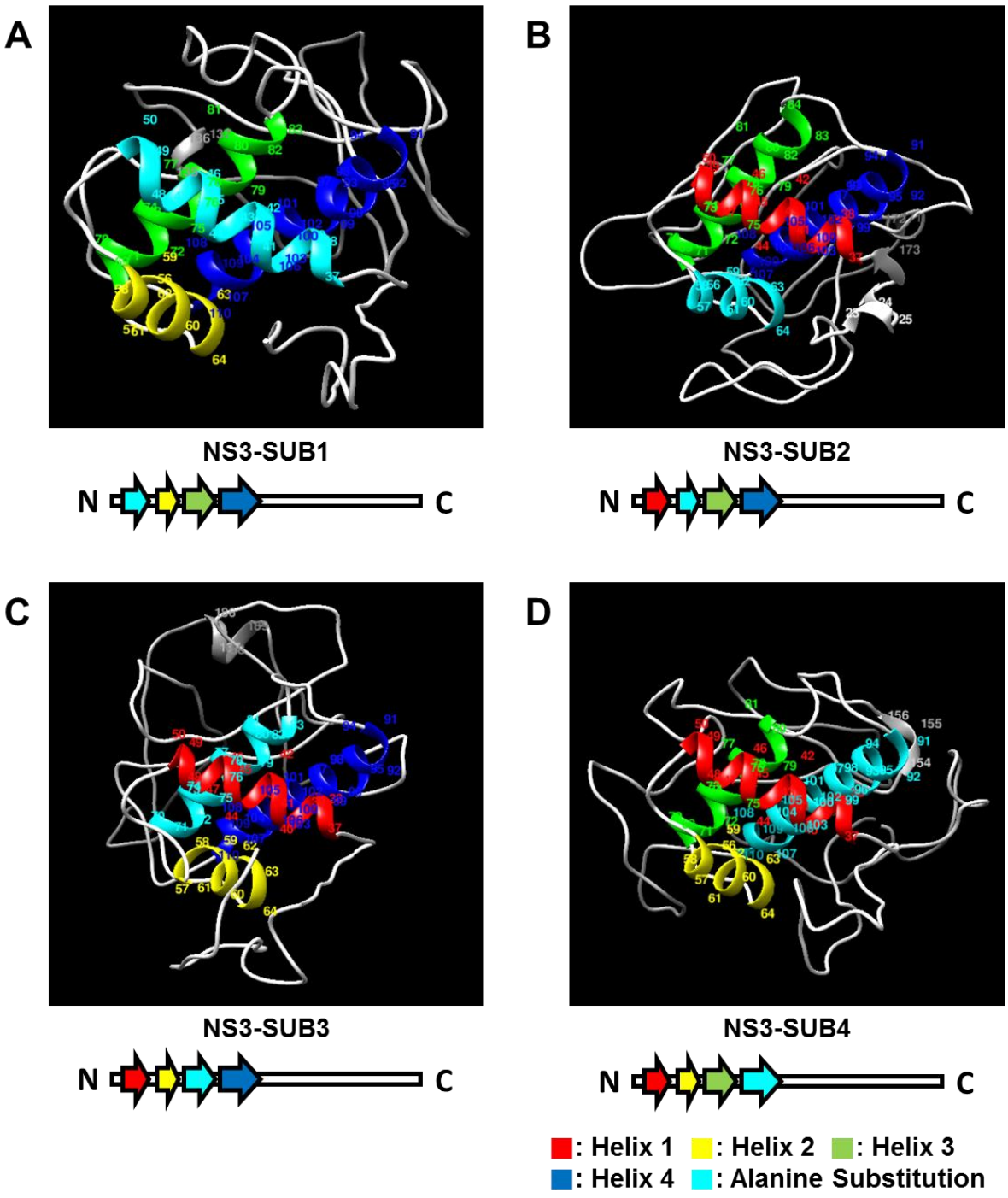

Fig. 2. Predicted 3D structure of alpha-helix alanine substitution mutants of NS3. (A) NS3-SUB1 was constructed by substituting helix 1 with alanines. (B) NS3-SUB2, (C) NS3-SUB3, and (D) NS3-SUB4 were also constructed for alpha-helix substitution with alanines.

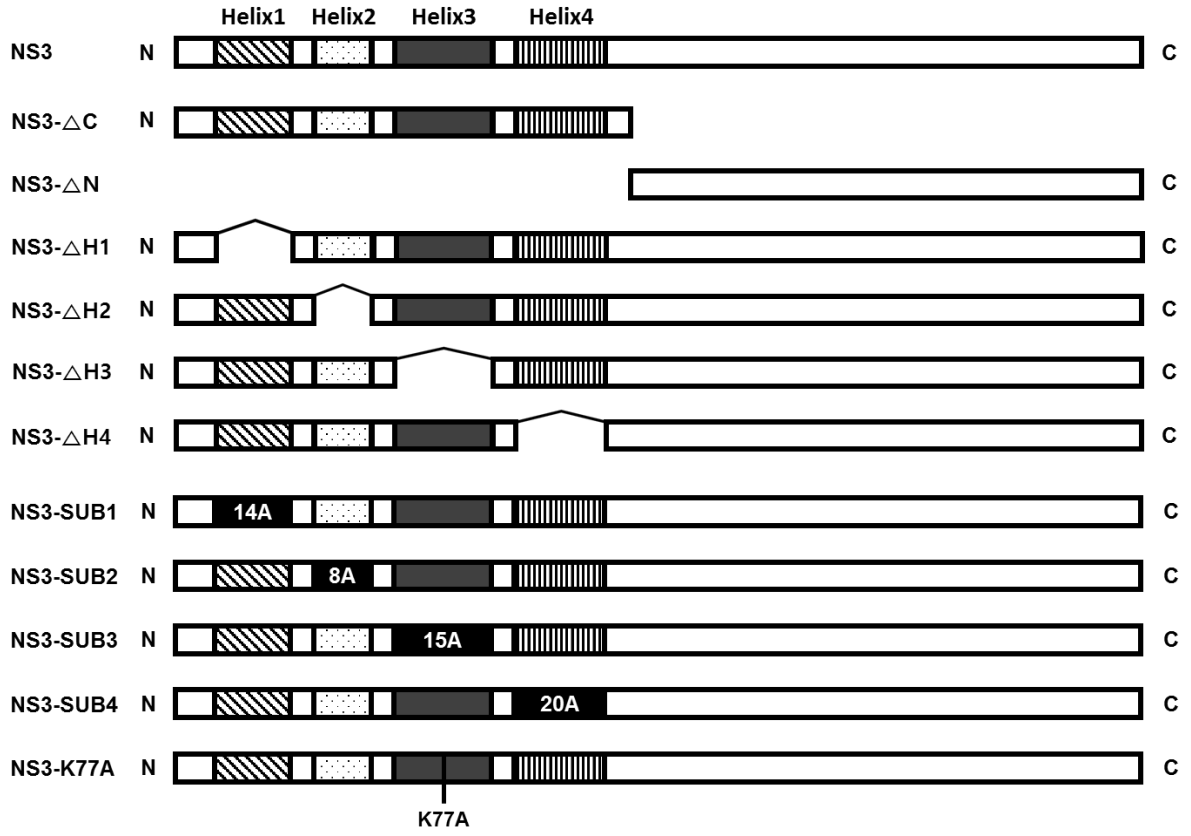

Fig. 3. Eleven mutated NS3 fragment constructs. All mutated NS3 fragments constructed by PCR from NS3 inserted pENTR/D-TOPO plasmid or by single joint PCR strategy. Six trancated NS3 mutants and five alanine substituted mutants were constructed.

3. Y2H analysis for identification of NS3 self-interaction site

Firstly, Y2H was conducted to investigate the interaction among the NS3-ΔC, NS3-ΔN and wild-type NS3 by testing three reporter genes (*HIS*3, *URA*3 and *lac*Z). For Y2H assay, pEXP32-NS3 (or mutated NS3s) and pEXP22-NS3 (or mutated NS3s) were constructed (Fig. 4A) and then two expression vectors, correspond to bait and prey, were co-transformed into MaV203. The results showed the self-interaction of NS3 full-length on SC-LTH+20mM 3AT medium (Fig. 5, left), but it did not grow on SC-LTU medium (Fig. 5, middle). This result indicates that the NS3 self-interaction is weaker interaction compared with the control of strong interaction (the interaction between Krev1 and RalGDS). In addtion, the interactions between NS3 and NS3-ΔC, and the self-interaction of NS3-ΔC were also detected. Especially, the interaction between NS3 and NS3-ΔC was detected on SC-LTU medium. This result showed that the interaction between NS3 and NS3-ΔC was stronger that NS3 self-interaction. In contrast, the interaction with NS3-ΔN mutant was not detectable in any combinations with NS3 full-length, NS3-ΔC and NS3-ΔN itself. These results indicate that the site of NS3 self-interactions is located on N-terminal part of NS3 peptide. The X-gal assay also showed the similar pattern in that the combination of NS3/NS3-ΔC (bait/prey) showed the strongest β-galactosidase expression (Fig 5, right). The other yeast transformants, such as NS3/NS3 and NS3-ΔC/NS3 also showed β-galactosidase activity.

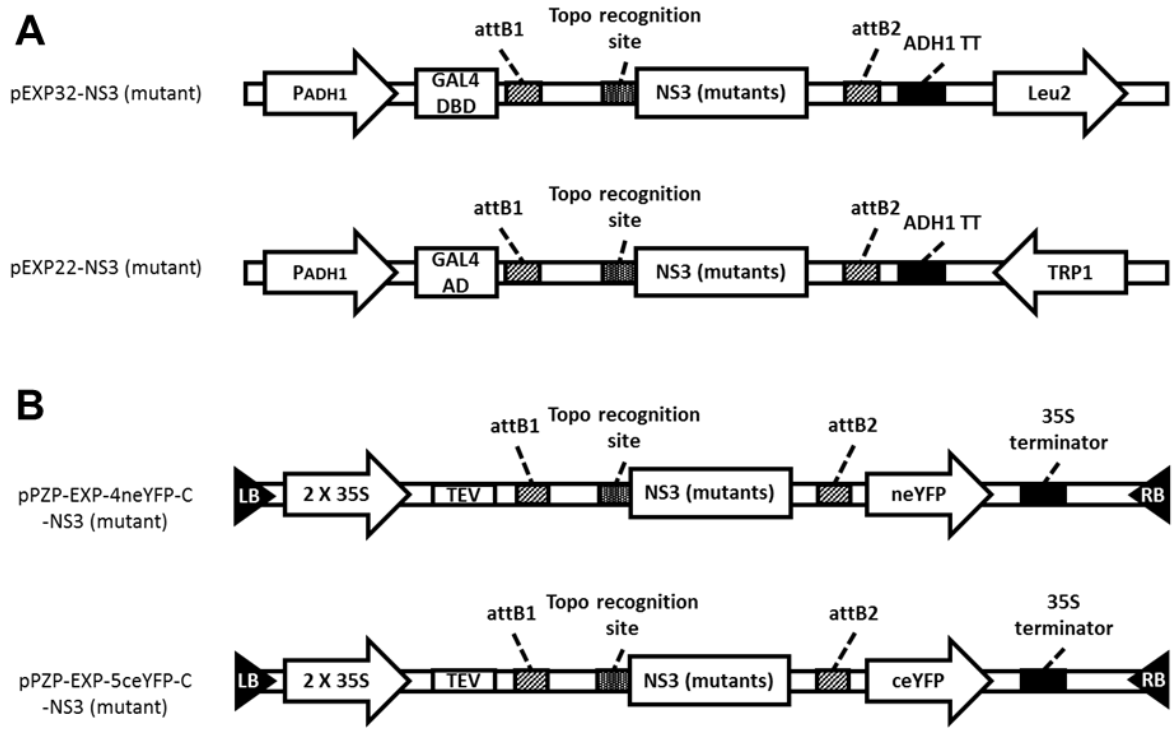

Fig. 4. Construction of expression vectors for interaction studies. (A) For Y2H clones, pEXP32-NS3 (mutated NS3s) and pEXP22-NS3 (mutated NS3s) were constructed by LR reaction between pENTR-NS3 (mutants) and pDEST32 or pDEST22 which contains GAL4 DNA binding domain (GAL4 DBD) or GAL4 activation domain (GAL4 AD), respectively. (B) For BiFC clones, NS3 and mutated NS3 were inserted in to pPZP-DEST-4neYFP-C and pPZP-DEST-5ceYFP-C by LR reaction, which was previously described.

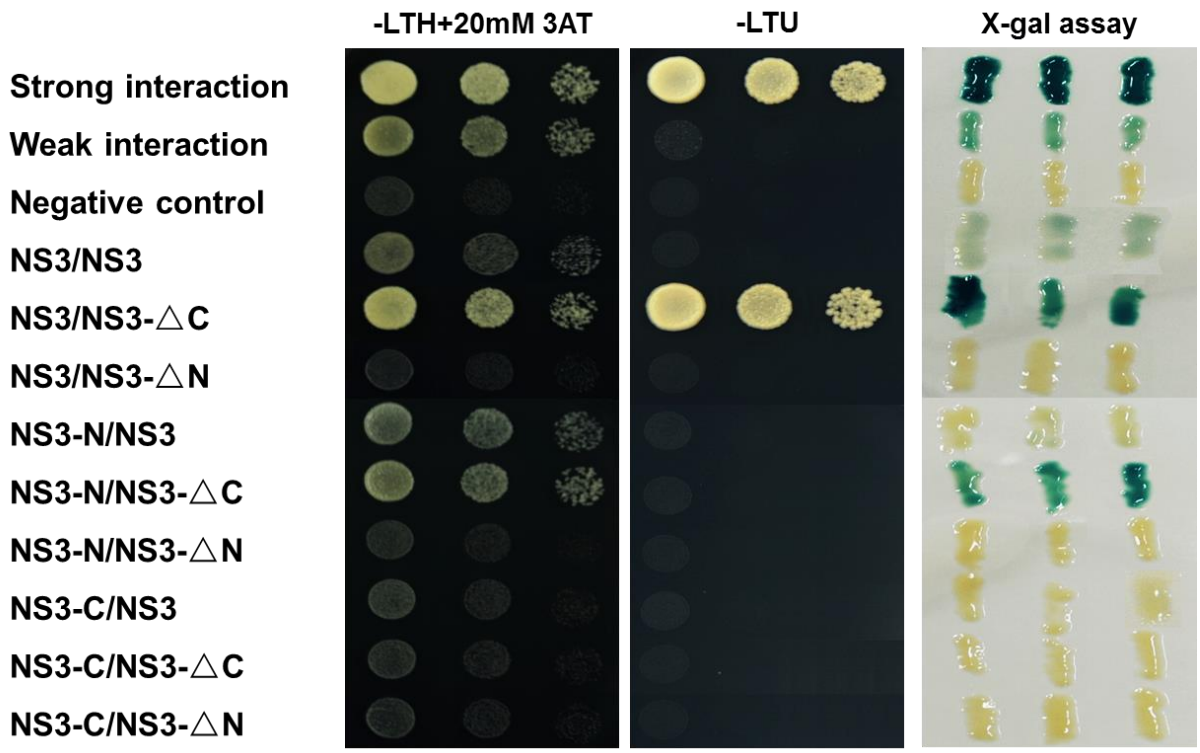

Fig. 5. Y2H assay among the NS3 full-length, NS3-ΔC and NS3-ΔN. Strong interaction is the positive control which represents strong interaction between pEXP32/Krev1 (bait) and pEXP22/RalGDS-wt (prey). Weak interaction represents the interaction between pEXP32/Krev1 (bait) and pEXP22/RalGDS-m1 (prey) and pEXP22/RalGDS-m2 was used as a prey of negative control.

4. BiFC assay for localization of NS3 self-interaction *in planta*

BiFC assay among the NS3-ΔC, NS3-ΔN and NS3 full-length was conducted to confirm previous Y2H results *in planta*. Because RSV CP and NS3 were already reported for its self-interaction (Lian et al., 2014), they were used as positive controls. Expression clones, which containing nYFP or cYFP (Fig. 4B), were co-inoculated into *N. benthamiana*, and YFP signal was investigated at two days post inoculation (dpi) with fluorecent microscopy. Under UV light, YFP signal was detected in CP/CP or NS3/NS3 inoculated leaves, which indicates the self-interaction of CP or NS3 *in planta*. In the same manner with Y2H result, YFP signal was detectable in NS3/NS3, NS3-ΔC/NS3-ΔC and all of combinations between NS3 full-length and NS3-ΔC (Fig 6). These results showed that the N-terminal region of NS3 contributes to NS3 self-interaction *in planta*, like Y2H result which is previously described. The level of YFP signal was slightly higher in NS3-ΔC self-interaction than NS3 full-length, and it is considered that the self-interaction of NS3-ΔC might be stronger than that of NS3 full-length. Constrastly, YFP signal was not detected in any combinations with NS3-ΔN, and it indicates that there is no interaction site on C-terminal region of NS3 peptide.

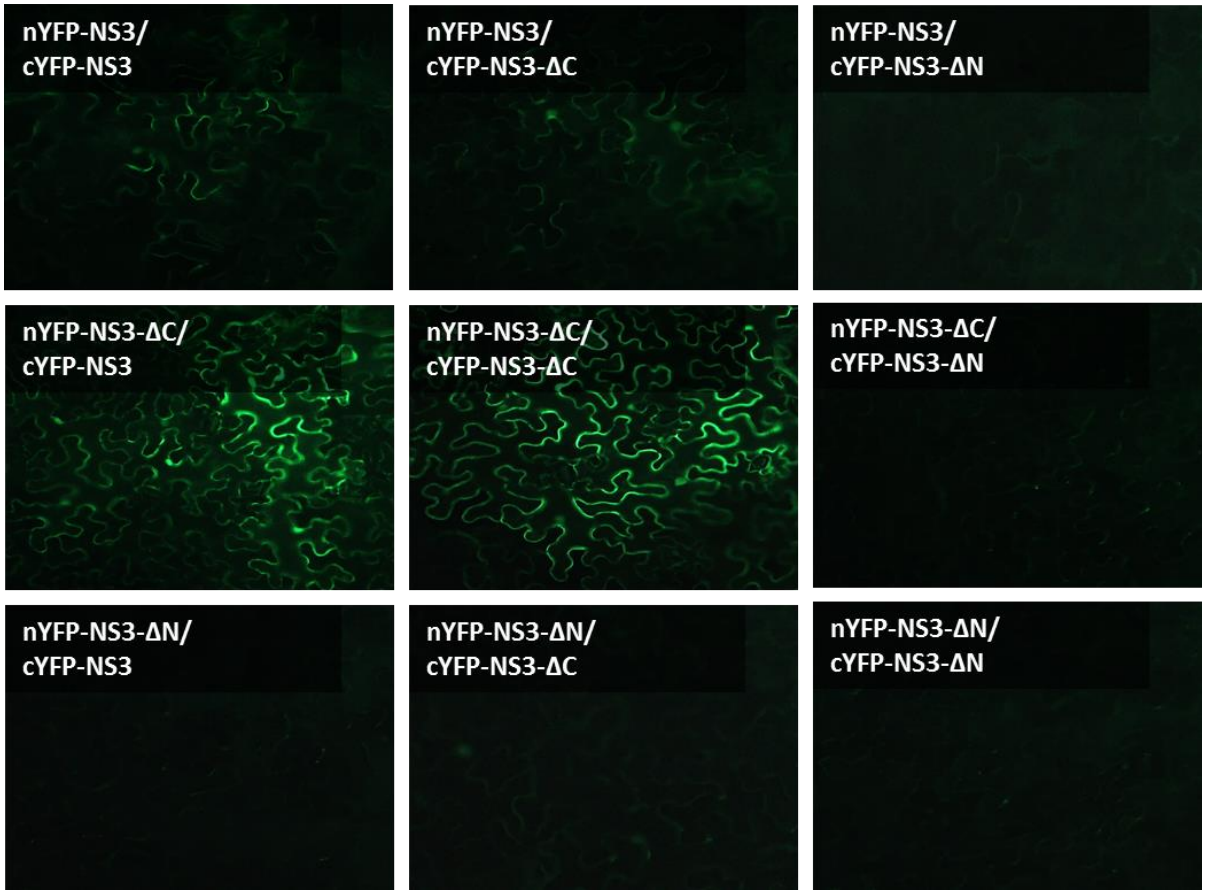

Fig. 6. BiFC assay among the NS3 full-length, NS3-ΔC and NS3-ΔN. nYFP-NS3/cYFP-NS3 was used as positive control, which already reported with with its self-interaction.

5. Identification of crucial motif for NS3 self-interaction in Y2H

To identify which alpha-helices are crucial motifs for NS3 self-interaction, Y2H assay were conducted with NS3 alpha-helix deletion mutants and alanine-substitution mutants. The results showed that all of the yeast transformants did not grow on SC-LTH+3AT or SC-LTU medium (Fig. 7). This result indicates that alpha-helix deletion mutants did not interact with wild-type NS3 or mutated NS3s. Furthermore, although four alpha-helix substitution mutants did not show the configurational changes on protein structure prediction model, they did not interact with wild type NS3 or mutated NS3s (Fig. 8). From these results, all of alpha-helices are considered to contribute to NS3 self-interaction and the residues on the alpha-helices might be necessary for self-interaction. In contrast, the yeast transformant with NS3-K77A/NS3 grew on SC-LTH+3AT medium (Fig. 8, right) and it indicates the weak interaction between NS3-K77A and wild-type NS3.

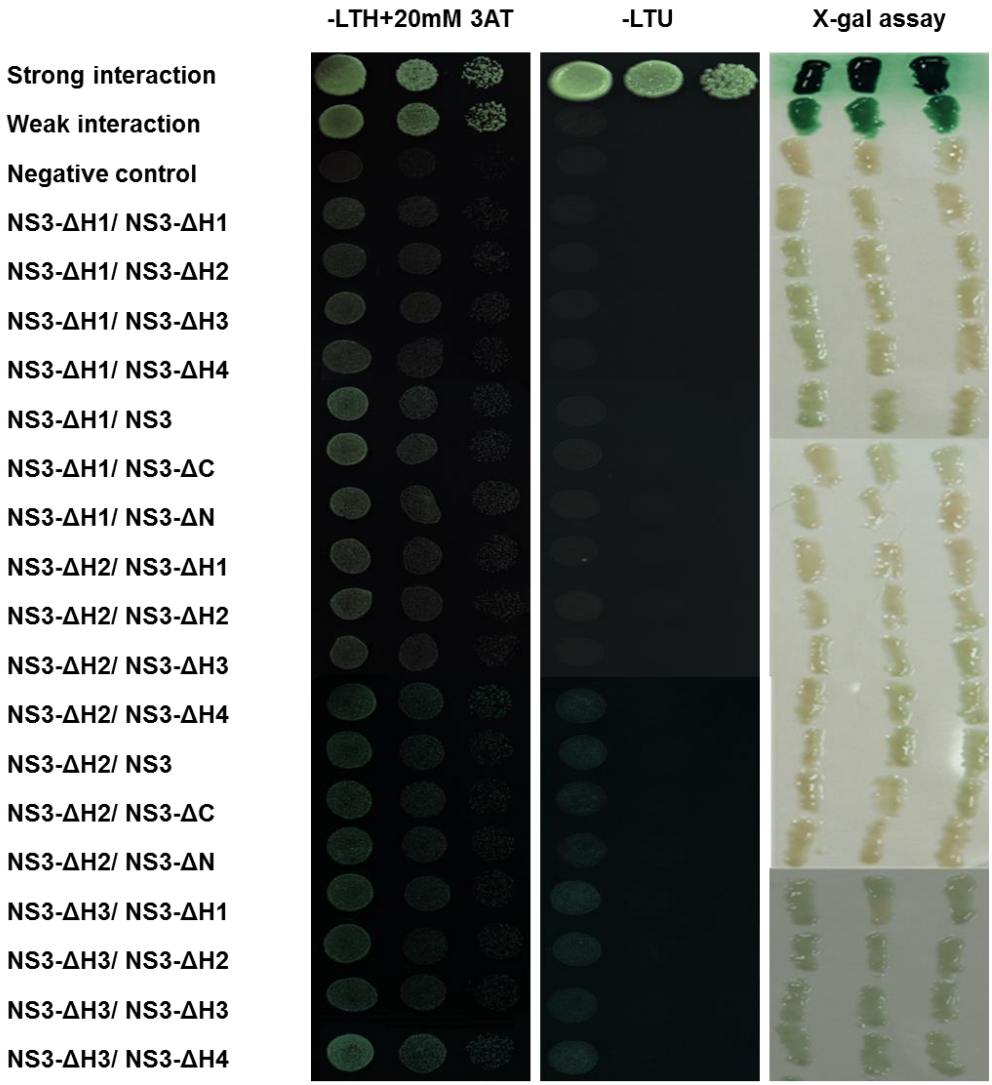

Fig. 7. Y2H assay of among the NS3 and NS3 deletion mutants.

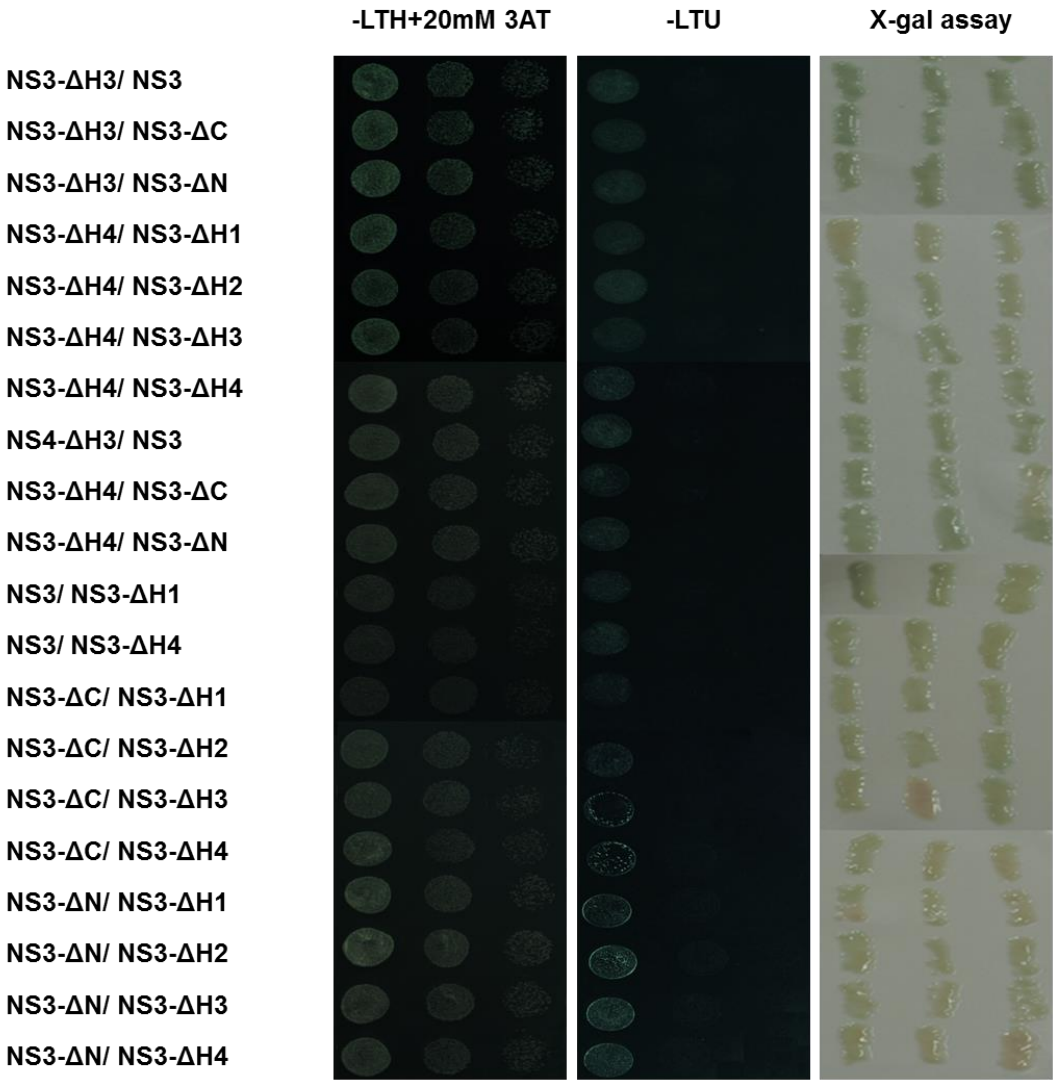

Fig. 7. Continued

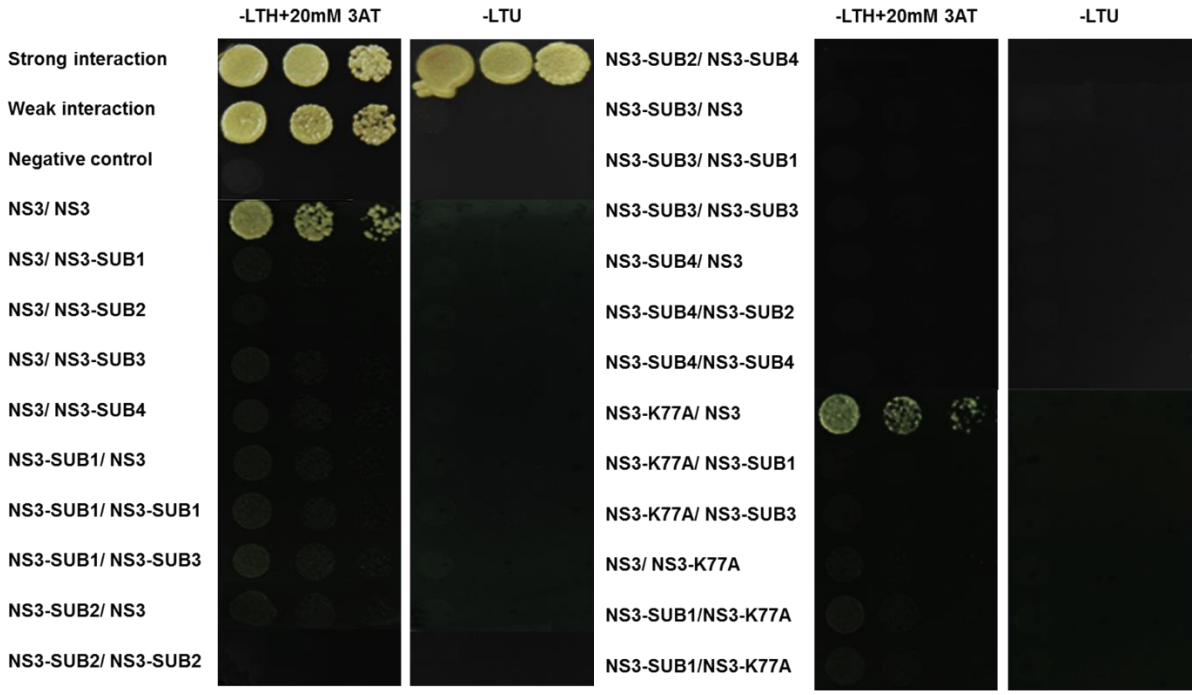

Fig. 8. Y2H assay among the NS3 and NS3 alanine substitution mutants.

6. Identification of crucial motifs for NS3 self-interaction *in planta*

To confirm previous Y2H results with alpha-helix deletion mutants and alanine substitution mutants *in planta*, BiFC assay was conducted with these mutated NS3s. The BiFC assay conducted with alpha-helix deletion mutants revealed that all of alpha-helix deletion mutants did not interact with NS3 full-length, NS-ΔC and NS-ΔN, so YFP signal was not detectable under UV light (Fig. 8). Likewise, YFP signal was not detected in every combination with alpha-helix substitution mutants (Fig. 9). These results also indicate that all of the alpha-helices are necessary for NS3 self-interaction *in planta*. However, in combinations between NS3 full-length and NS3-K77A, YFP signal was detected. Particularly, the co-inoculation of NS3-K77A-nYFP clone and NS3-K77A-cYFP clone showed high level of YFP signal in nucleus. It is considered that a point mutation on K77 result in localizational change (Fig. 10, lower left).

Fig. 9. BiFC assay between NS3 and alpha-helix deleted NS3 mutants.

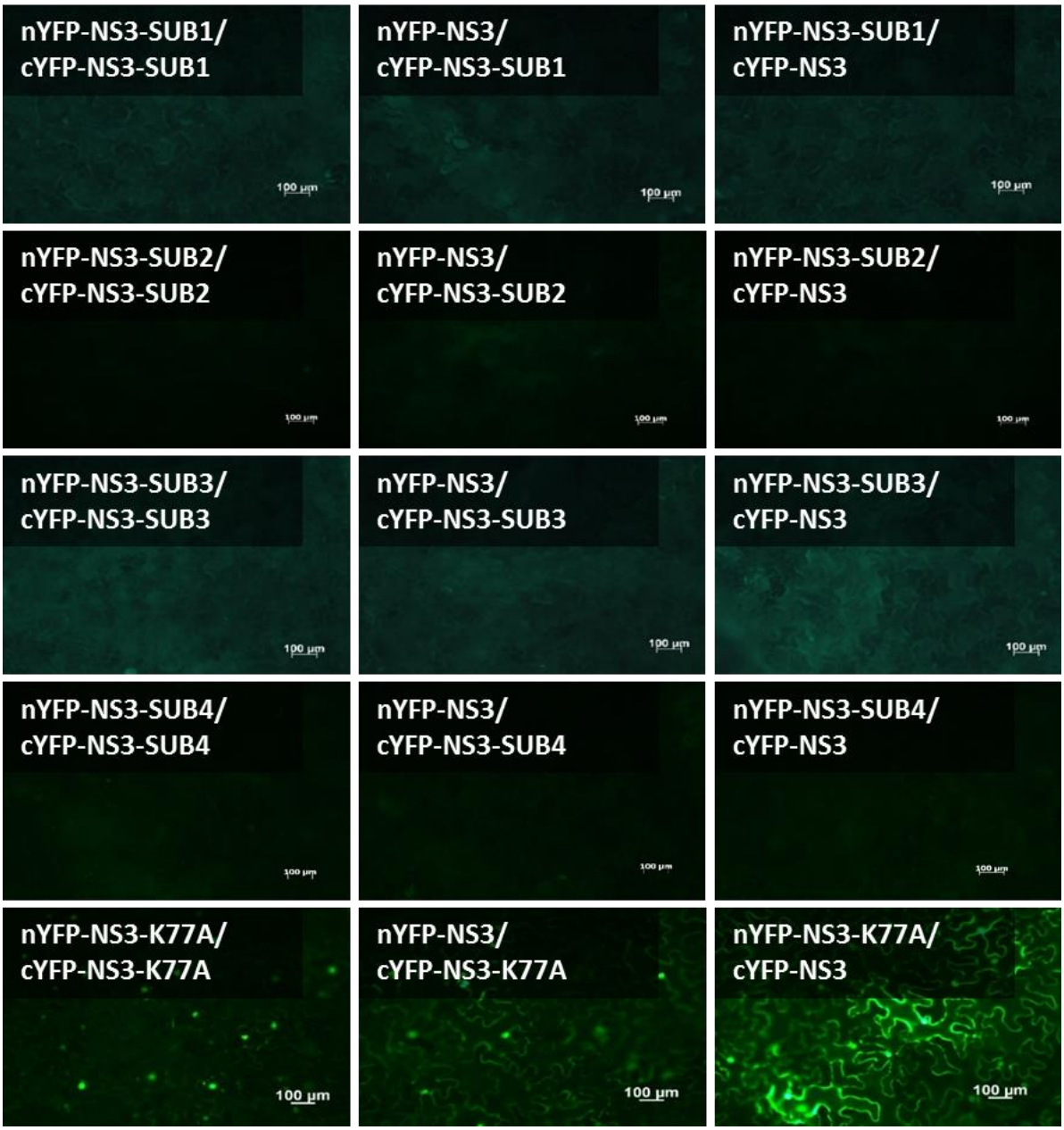

Fig. 10. BiFC assay of NS3 and NS3 alanine substitution mutants.

7. RNA silencing suppression analysis

To identify the relationship between NS3 self-interaction and silencing suppressor activity, the function of mutated NS3s was investigated by inducing GFP silencing in *N. benthamiana*. For over-expression of NS3 and mutated NS3s, pMDC32 expression vector which containing dual 35S promoter was used (Fig. 11, upper) and pCAMBIA-Hairpin GFP vector was also constructed for GFP silencing (Fig. 11, lower). To optimize the condition of GFP silencing and silencing suppression, two methods were designed and examined. One method is to express NS3 after GFP over-expression (GFP-VSR method), and the other is to express NS3 before GFP over-expression (VSR-GFP method). Three days after inoculation of GFP over-expression clone, the spots, where NS3 (or NS3 mutants) were over-expressed by agro-infiltration, were investigated under UV light. When applying VSR-GFP method, GFP silencing was sucessfully induced in the spot where hairpin GFP over-expression clone had inoculated and GFP silencing suppression by P19 and NS3 was also detected (Fig. 12). Therefore, VSR-GFP method was used for GFP silencing suppression analysis of mutated NS3s.

The result showed that P19, a positive control as a silencing suppressors, sucessfully suppressed host GFP silencing mechanism, so the GFP signal was detected in P19-expressed spot. The NS3 also suppressed GFP silencing and GFP was detected in NS3-expressed spot (Fig 13, upper).

To identify the relationship between NS3 self-interaction and silencing suppressor activity, GFP silencing suppression analysis of mutated NS3s was also conducted. Firstly, four alpha-helix deletion mutants, which lost its self-interaction ability in Y2H or BiFC assay, was not able to suppress GFP silencing, so GFP signal was disappeared and red spots were formed. Likewise, four alpha-helix substitution mutants, which also lost its self-interaction ability,

could not suppress GFP silencing, so GFP was silenced (Fig 13, middle).

In the case of NS3-K77A substitution mutant, which showed self-interaction in Y2H and BiFC, inhibited GFP silencing, and GFP signal was detected in this area. This result indicated that NS3-K77A successfully suppressed the GFP silencing which is activated by GFP hairpin construct. However NS3-ΔC mutant, which also showed self-interaction in Y2H or BiFC assay, lost its silencing suppressor activity, and GFP signal was disappeared in this spot. NS3-ΔN mutant, which did not showed the self-interaction, also could not suppress GFP silencing (Fig 13, lower).

Overall results of RNA silenging suppression analysis indicate that the mutated NS3s, which can not interact itself, lost its silencing suppressor activity, and the NS3-ΔC mutant also can not suppress GFP silencing. Only the NS3-K77A mutant, which can interact itself and contains intact C-terminal region, repressed GFP silencing in *N. benthamiana*.

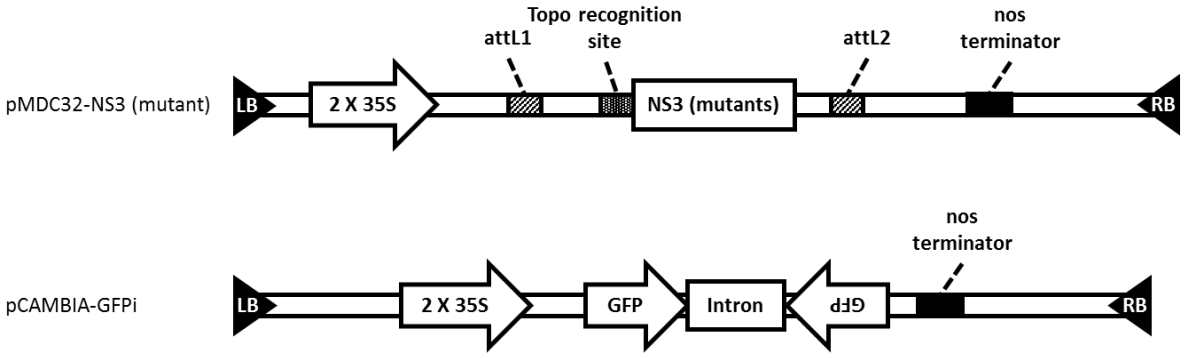

Fig. 11. Vector construction for over-expression of NS3 or mutated NS3s and for GFP silencing.

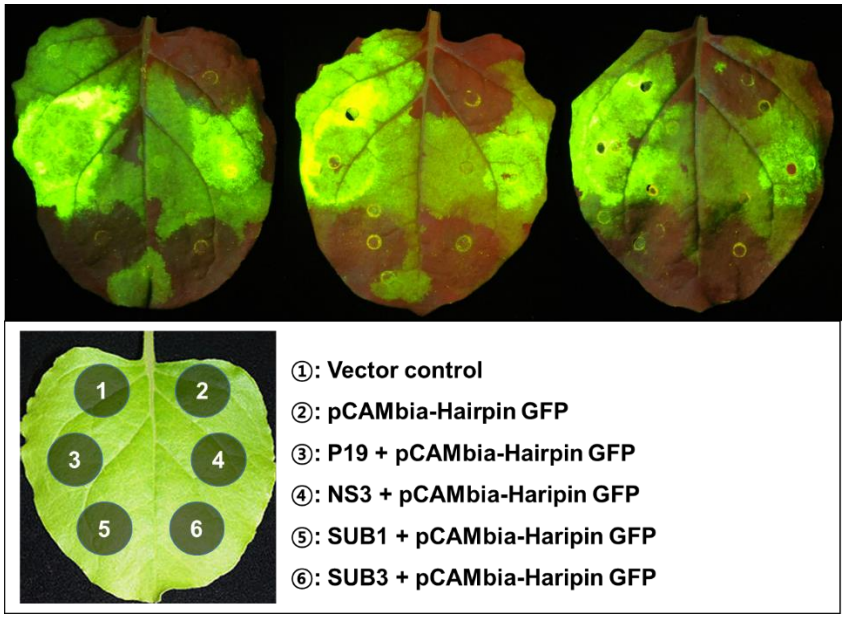

Fig. 12. Examination of GFP silenging construct in *N. benthamiana*

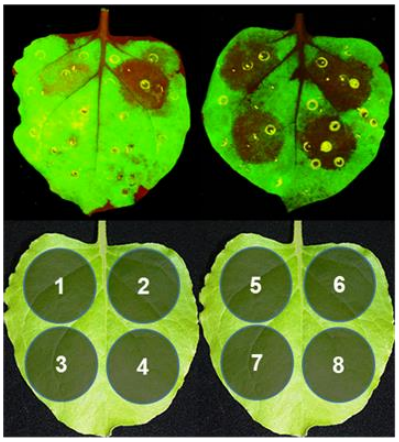

	Y2H	BiFC	Suppressor Activity
NS3-ΔH1	-	-	-
NS3-ΔH2	-	-	-
NS3-ΔH3	-	-	-
NS3-ΔH4	-	-	-

①: pMDC32, ②: GFPi, ③: p19 + GFPi, ④: NS3 + GFPi, ⑤-⑧: NS3-ΔH1-4 + GFPi

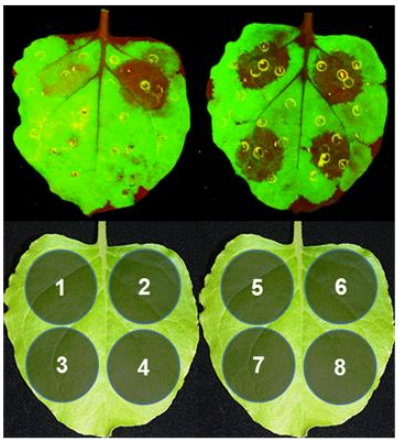

	Y2H	BiFC	Suppressor Activity
NS3-SUB1	-	-	-
NS3-SUB2	-	-	-
NS3-SUB3	-	-	-
NS3-SUB4	-	-	-

①: pMDC32, ②: GFPi, ③: p19 + GFPi, ④: NS3 + GFPi, ⑤-⑧: NS3-SUB1-4 + GFPi

	Y2H	BiFC	Suppressor Activity
NS3-K77A	+	+	+
NS3-ΔC	+	+	-
NS3-ΔN	-	-	-

①: pMDC32, ②: GFPi, ③: p19 + GFPi, ④: NS3 + GFPi, ⑤: NS3-K77A + GFPi, ⑥: NS3-ΔC + GFPi, ⑦: NS3-ΔN + GFPi

Fig. 13. RNA silencing suppresssion analysis of mutated NS3s.

Discussion

In this study, computational analysis was conducted to predict 3D structure of NS3 and identified four alpha-helices on N-terminal region of the NS3. Furthermore, the interaction study among the NS3, NS3-ΔC and NS3-ΔN showed that the crucial motif of NS3 self-interaction exist in N-terminal region of NS3. Since the importance of alpha-helices in protein-protein interactions have been reported (Azzarito et al., 2013), I generated mutants including alpha-helix deletion and substitution mutants to determine importance of alpha-helix structures for NS3 self-interaction.

The interaction study based on Y2H and BiFC assay showed that all of four alpha-helix structures are important for NS3 self-interaction. Considering that the alpha-helice are involved in numerous protein-protein interaction in nature, it is supposed that these four alpha-helices directly or indirectly contribute to NS3 self-interaction. For example, it was reported that the polymerization of hepatitis B virus capsid protein is caused by the bundle formation of four alpha-helices (Conway et al., 1997). In this case, two pairs of alpha-helices directly interact and contribute to polymerization of capsid protein. *Tombusvirus* P19 also forms a dimer to function as a gene silencing suppressor. Dimerization of this protein is mediated by the interaction between alpha-helix and beta-sheet structures (Ye et al., 2003). Besides, numerous protein-protein interactions mediated with alpha-helix motifs were reported, so I consider the alpha-helix structure of NS3 might be key motif for its self-interaction.

NS3-K77A, whose lysine77 is substituted to alanine, showed self-interaction in Y2H and BiFC assay suggesting that the electric charge of alpha-helix 3 might not be the major factor for NS3 self-interaction. However, NS3-K77A mutation resulted in nuclear localization when

expressed *in planta*. Compared to wild-type NS3, the expression level of YFP in nucleus was much higher with NS3-K77A and the YFP signal in cytosol was weaker. It is expected that the mutation on K77 affects to the localization of NS3. Subcellular localization studies are required to confirm this result.

Additionally, analysis of GFP silencing suppressor activity showed that the close relationship between NS3 self-interaction and the function as a viral suppressor of RNA silencing. Four alpha-helix deletion mutants, four alpha-helix substitution mutants and NS3-ΔN which lost NS3 self-interaction ability did not suppress GFP silencing in *N. benthamiana*. In contrast, NS3-K77A which interact itself or NS3 full-length successfully suppress the GFP silencing. In case of NS3-ΔC, however, did not suppress GFP silencing inspite of its self-interaction ability. This result indicate that NS3 self-interaction might be prerequisite to NS3 function as RNA silencing suppressor.

Until now, various VSRs have been reported and their mechanisms about suppression of RNA silencing also have been studied (Guo et al., 2014). The TBSV viral protein P19 is the most well known VSR and it function as RNA silencing suppressor by composing dimer. Furthermore, NS3 protein of RHBV which belongs to *Tenuivirus*, the genus including RSV, also form dimer for function of VSR (Hemmes et al., 2007). P5 protein of rice grassy stunt virus (RGSV), which is also a member of genus *Tenuivirus*, showed self-interaction (Chomchan et al., 2003). Judging by the dimer conformation of RHBV NS3 for silencing suppressor activity and self-interaction ability of RGSV, it is plausible to speculate that the RSV NS3 also forms homodimer for its silencing suppressor activity.

On the other hand, NS3-ΔC mutant did not show its silencing suppressor activity in spite of

its self-interaction ability. I assumed that the functional domain of NS3 was removed in NS3-ΔC. Previously, researches about siRNA binding activity of various VSRs have been conducted. For example, Carnation Italian ringspot virus (CIRV) p19 protein directly binds to siRNA and acts as VSR (Baulcombe & Molnár, 2004). Furthermore, in case of RHBV NS3, it contains siRNA binding site on C-terminal portion of peptide. By computational analysis, the siRNA binding site of RHBV NS3 was also conserved at the C-terminal region of RSV NS3 (Fig. 14). Therefore, it is possible that the RSV NS3 also contains siRNA binding site at the C-terminal region and thus lost its silencing suppressor activity despite of its self-interaction ability.

In summary, I identified the crucial motif of NS3 required for its self-interaction. Based on protein 3D structure prediction model, I assumed four alpha-helices located at the N-terminal region as essencial motif for maintainging NS3 self-interaction. In addtion, I also tested RNA silencing suppression activity of RSV NS3 by conducting GFP silencing assay. The result showed that only the NS3-K77A mutant, which has self-interaction ability and contain presumed siRNA binding site, successfully suppress the GFP silenging. These results indicate that the NS3 self-interaction might be prerequisite for its silencing suppressor activity.

Fig. 14. Comparative analysis of sequences between RSV and RHBV NS3s.

LITERATURE CITED

Azzarito, V., Long, K., Murphy, N. S., Wilson, A. J. (2013). Inhibition of [alpha]-helix-mediated protein-protein interactions using designed molecules. *Nature chemistry, 5*(3), 161-173.

Baulcombe, D. C., Molnár, A. (2004). Crystal structure of p19–a universal suppressor of RNA silencing. *Trends in biochemical sciences*, 29(6), 279-281.

Chomchan, P., Li, S.-F., Shirako, Y. (2003). Rice grassy stunt tenuivirus nonstructural protein p5 interacts with itself to form oligomeric complexes in vitro and in vivo. *Journal of virology, 77*(1), 769-775.

Conway, J., Cheng, N., Zlotnick, A., Wingfield, P., Stahl, S., Steven, A. (1997). Visualization of a 4-helix bundle in the hepatitis B virus capsid by cryo-electron microscopy. *Nature*, 386, 91-94

Danielson, D. C., Pezacki, J. P. (2013). Studying the RNA silencing pathway with the p19 protein. *FEBS letters, 587*(8), 1198-1205.

Du, Z., Xiao, D., Wu, J., Jia, D., Yuan, Z., Liu, Y., Hu, L., Han, Z., Wei, T., Lin, Q., Wu, Z., Xie, L. (2011). p2 of rice stripe virus (RSV) interacts with OsSGS3 and is a silencing suppressor. *Molecular plant pathology, 12*(8), 808-814.

Edwards, T. A., Wilson, A. J. (2011). Helix-mediated protein–protein interactions as targets for intervention using foldamers. *Amino acids, 41*(3), 743-754.

Guo, D., Rajamäki, M.-L., Saarma, M., Valkonen, J. P. (2001). Towards a protein interaction map of potyviruses: protein interaction matrixes of two potyviruses based on the yeast two-hybrid system. *Journal of general virology, 82*(4), 935-939.

Guo, W., Liew, J. Y., Yuan, Y. A. (2014). Structural insights into the arms race between host and virus along RNA silencing pathways in Arabidopsis thaliana. *Biological Reviews, 89*(2), 337-355.

Hayano, Y., Kakutani, T., Hayashi, T., Minobe, Y. (1990). Coding strategy of rice stripe virus: major nonstructural protein is encoded in viral RNA segment 4 and coat protein in RNA complementary to segment 3. *Virology*, 177(1), 372-374.

Hemmes, H., Kaaij, L., Lohuis, D., Prins, M., Goldbach, R., Schnettler, E. (2009). Binding of small interfering RNA molecules is crucial for RNA interference suppressor activity of rice hoja blanca virus NS3 in plants. *Journal of general virology, 90*(7), 1762-1766.

Hemmes, H., Lakatos, L., Goldbach, R., Burgyán, J., Prins, M. (2007). The NS3 protein of Rice hoja blanca tenuivirus suppresses RNA silencing in plant and insect hosts by efficiently binding both siRNAs and miRNAs. *Rna,*

13(7), 1079-1089.

Lian, S., Cho, W. K., Jo, Y., Kim, S.-M., Kim, K.-H. (2014). Interaction study of rice stripe virus proteins reveals a region of the nucleocapsid protein (NP) required for NP self-interaction and nuclear localization. *Virus Research, 183*, 6-14.

Lian, S., Jonson, M. G., Cho, W.-K., Choi, H.-S., Je, Y.-H., Kim, K.-H. (2011). Generation of antibodies against Rice stripe virus proteins based on recombinant proteins and synthetic polypeptides. *The Plant Pathology Journal, 27*(1), 37-43.

Morrison, K. L., Weiss, G. A. (2001). Combinatorial alanine-scanning. *Current opinion in chemical biology*, 5(3), 302-307.

Park, J.-W., Faure-Rabasse, S., Robinson, M. A., Desvoyes, B., Scholthof, H. B. (2004). The multifunctional plant viral suppressor of gene silencing P19 interacts with itself and an RNA binding host protein. *Virology, 323*(1), 49-58.

Pringle, C. (1998). The universal system of virus taxonomy of the International Committee on Virus Taxonomy (ICTV), including new proposals ratified since publication of the Sixth ICTV Report in 1995. *Archives of virology, 143*(1), 203-210.

Pumplin, N., Voinnet, O. (2013). RNA silencing suppression by plant pathogens:

defence, counter-defence and counter-counter-defence. *Nature Reviews Microbiology, 11*(11), 745-760.

Qu, Z., Liang, D., Harper, G., Hull, R. (1997). Comparison of sequences of RNAs 3 and 4 of rice stripe virus from China with those of Japanese isolates. *Virus Genes, 15*(2), 99-103.

Reddy, T. R. (2000). A single point mutation in the nuclear localization domain of Sam68 blocks the Rev/RRE-mediated transactivation. *Oncogene*, 19(27), 3110-3114.

Wang, M.-B., Masuta, C., Smith, N. A., Shimura, H. (2012). RNA silencing and plant viral diseases. *Molecular Plant-Microbe Interactions, 25*(10), 1275-1285.

Wu, S.-J., Zhong, H., Zhou, Y., Zuo, H., Zhou, L.-H., Zhu, J.-Y., Ji, C.-Q., Gu, S.-L., Gu, M.-H., Liang, G.-H. (2009). Identification of QTLs for the resistance to rice stripe virus in the indica rice variety Dular. *Euphytica, 165*(3), 557-565.

Wu, G., Lu, Y., Zheng, H., Lin, L., Yan, F., Chen, J. (2013). Transcription of ORFs on RNA2 and RNA4 of Rice stripe virus terminate at an AUCCGGAU sequence that is conserved in the genus Tenuivirus. *Virus research*, 175(1), 71-77.

Wu, W., Zheng, L., Chen, H., Jia, D., Li, F., Wei, T. (2014). Nonstructural protein

NS4 of Rice stripe virus plays a critical role in viral spread in the body of vector insects. *PLoS One, 9*(2), e88636.

Xiong, R., Wu, J., Zhou, Y., Zhou, X. (2009). Characterization and subcellular localization of an RNA silencing suppressor encoded by Rice stripe tenuivirus. *Virology, 387*(1), 29-40.

Ye, K., Malinina, L., Patel, D. J. (2003). Recognition of small interfering RNA by a viral suppressor of RNA silencing. *Nature*, 426(6968), 874-878.

Zhang, C., Wu, Z., Li, Y., Wu, J. (2015). Biogenesis, Function, and Applications of Virus-Derived Small RNAs in Plants. *Frontiers in microbiology, 6*, 1237

Zhao, S., Hao, J., Xue, Y., Liang, C. (2015). Intracellular localization of rice stripe virus RNA-dependent RNA polymerase and its interaction with nucleocapsid protein. *Virus Genes, 51*(3), 423-429.

Rice stripe virus 단백질 NS3 의 자가상호작용과 유전자 침묵 억제 기능에 중요한 아미노산 및 도메인의 동정

김한길

초록

벼줄무늬잎마름병 (RSV) 바이러스는 *Tenuivirus* 속에 속하는 바이러스로써 벼 재배에 있어 가장 위험한 바이러스 중 하나로 알려져 있다. 이 RSV의 게놈은 4개의 단가닥 RNA들로 이루어져 있으며 이들은 총 7개의 단백질들을 암호화하고 있다. 이들 중 RNA 분절 3에 암호화 되어 있는 NS3 단백질은 유전자 침묵 억제 인자로써 기존에 이미 그 기능이 밝혀진 바 있는 단백질이며 이는 또한 자가상호작용을 통해 유전자 침묵 억제 작용을 수행하는 것으로 알려져 있다. 본 연구팀은 이러한 NS3의 자가 상호작용에 중요한 아미노산 잔기 또는 도메인을 동정하고자 단백질 3차 구조 예측 프로그램을 이용하였으며 이 모델을 기반으로 하여 4개 알파헬릭스 삭제 돌연변이와 4개 알파헬릭스를 각각 알라닌으로 치환한 NS3 돌연변이를 포함하여 총 11개의 NS3 돌연변이 클론을 제작하였다. 이후 이렇게 제작된 돌연변이들을 이용하여 yeast-two hybrid (Y2H)와 bimolecular fluorescence complementation (BiFC) assay를 이용한 이들의 상호작용을 연구하였다. 그 결과 NS3의 N 말단 부분의 펩타이드 서열이 NS3의 상호작용에 관여한다는 것을 확인할 수 있었다. 또한 4개의 알파헬릭스 삭제 돌연변이 그리고 4개 알파헬릭스를 각각 알라닌으로 치환한 돌연변이들을 이용한 Y2H와 BiFC assay 실험 결과 이들은 자가 상호작용 능력을 상실하는 것으로 확인되었다. 또한 본 연구팀은 이러한 NS3의 자가상호작용이 유전자 침묵 억제 기

능과 어떠한 연관성을 가지는지에 대해 연구하기 위하여 Agrobacterium을 이용한 각 NS3 돌연변이의 일시적 과발현 및 GFP 침묵 방법을 이용하여 유전자 침묵 억제 기능을 조사하였다. 그 결과 4개 알파헬릭스 삭제 돌연변이와 4개의 알파헬릭스 알라닌 치환 돌연변이의 경우 유전자 침묵 억제 기능을 상실하였으며 자가 상호작용이 확인되었던 77번 라이신을 알라닌으로 치환한 돌연변이의 경우에만 유전자 침묵 억제 기능이 확인되었다. 이러한 결과들을 종합해볼 때, 이러한 NS3의 자가 상호작용이 기주의 RNA 침묵에 대한 유전자 침묵 억제 기작에 필수적인 것이라 여겨진다.

주요어: 벼줄무늬잎바이러스, 단백질 3차 구조 예측, RNA 침묵, 유전자 침묵 억제인자, 단백질 상호작용, GFP 침묵